Denitrogenation process in $ThMn_{12}$ nitride by *in situ* neutron powder diffraction

A. Aubert,[1,*] I. Puente-Orench,[2,3,†] J. M. Porro,[1,4] S. Luca,[5] J. S. Garitaonandia,[6] J. M. Barandiaran,[6] and G. C. Hadjipanayis[7]

[1]*Basque Center for Materials, Applications and Nanostructures (BCMaterials), Leioa, Spain*
[2]*Instituto Nanociencia y Materiales de Aragón (INMA) CSIC-Universidad de Zaragoza, Spain*
[3]*Institut Laue-Langevin, Grenoble, France*
[4]*Ikerbasque, the Basque Foundation for Science, Bilbao, Spain*
[5]*Univ. Grenoble Alpes, CEA LITEN, DTNM, LMCM, Grenoble, France*
[6]*Faculty of Science and Technology, University of the Basque Country (UPV/EHU), Leioa, Spain*
[7]*Department of Physics and Astronomy, University of Delaware, Newark, Delaware 19716, USA*

(Received 27 September 2020; revised 17 December 2020; accepted 12 January 2021; published 29 January 2021)

$ThMn_{12}$ nitrides are good candidates for high performance permanent magnets. However, one of the remaining challenges is to transfer the good properties of the powder into a useful bulk magnet. Thus, understanding the denitrogenation process of this phase is of key importance. In this study, we investigate the magnetic and structural stability of the $(Nd_{0.75}, Pr_{0.25})_{1.2}Fe_{10.5}Mo_{1.5}N_x$ compound ($x = 0$ and 0.85) as function of temperature by means of neutron powder diffraction. Thermal dependence of the lattice parameters, formation of α-(Fe,Mo), as well as the nitrogen content in the nitrides are investigated by heating the compounds up to 1010 K. The decomposition takes place mainly via the formation of the α-(Fe,Mo) phase, which starts at around 900 K, whereas the nitrogen remains stable in the lattice. Additionally, we show that the magnetic properties of the nitrides [$M(4\ \mathrm{T}) = 90\ \mathrm{Am^2/kg}$ and $H_c = 0.55$ T] are maintained after the thermal treatments up to 900 K. This study demonstrates that the $ThMn_{12}$ nitrides with the Mo stabilizing element offer good prospects for a bulk magnet provided an adequate processing route is found.

DOI: 10.1103/PhysRevMaterials.5.014415

I. INTRODUCTION

The critical and strategic character of rare earth (RE) elements as raw materials has motivated a renewed interest in the search for rare-earth-lean and rare-earth-free hard magnetic materials for permanent magnet applications. The tetragonal $R(Fe,M)_{12}$ (R = rare earth, M = transition metal) compounds with the $ThMn_{12}$ structure (1:12) have recently shown a great potential to fulfill the criteria for future permanent magnets [1–3].

Nd-based 1:12 structures have a weak net anisotropy field (<1 T) at room temperature as it is predominantly determined by the Fe-sublattice anisotropy [4,5]. However, adding an interstitial light element (e.g., N or C) modifies the unit cell without changing the symmetry of the parent compound; this changes the Fe-Fe interaction and establishes a strong positive crystal field coefficient A_{20} at the Nd(2a) site, which is effective to create a large uniaxial magnetic anisotropy [6,7]. The inclusion of such light elements is performed by the gas-phase interstitial modification process, which consists of heating the parent compound under the desired gas atmosphere (e.g., nitrogen) for a certain time which allows the gas-solid reaction to occur [8–10]. This process has also been studied by *in situ* neutron diffraction, which is an excellent way to evaluate the reaction dynamics in real time, as neutrons are sensitive to light elements (e.g., H, C, N) [11–13].

Even though powder nitrides have recently shown success in obtaining hard magnetic properties [14,15], one of the remaining challenges is to transfer the good properties of the powder into a useful bulk magnet [16,17]. One weakness of the $ThMn_{12}$ nitrides is their tendency to disproportionate or eventually denitrogenate at temperatures which are required for sintering [18]. After a certain temperature is reached, one can expect an irreversible decomposition into other stable phases, like α-Fe or NdN, which limits the possibility of converting the hard magnetic properties of the nitrogenated powder into a dense permanent magnet [8,9]. Thus, understanding the thermostability of this phase is of key importance.

In the present study, we investigate the denitrogenation and decomposition process of $(Nd_{0.75}, Pr_{0.25})_{1.2}Fe_{10.5}Mo_{1.5}N_x$ with the $ThMn_{12}$ structure. A mixture of $Nd_{0.75}Pr_{0.25}$ (i.e., didymium) is used instead of pure Nd or Pr because it is less expensive since it requires less processing during the extraction of rare-earth elements [19]. Here, we first investigate the structural and magnetic properties of the parent compound and its nitride to ensure that appropriate nitrogenation occured. Then, we study the temperature-induced structural changes up to 1100 K by neutron powder diffraction of both compounds. It is worth mentioning that the $ThMn_{12}$ nitrides show excellent phase stability up to high temperatures

*Present address: Functional Materials, TU Darmstadt, 64287, Darmstadt, Germany; aubert.alex@outlook.fr
†puenteorench@ill.fr

 ©2021 American Physical Society

(<930 K), which is attributed to an appropriate nitrogenation process and the use of Mo as a stabilizing element. Finally, we show that the magnetic properties of the nitrides are maintained after thermal treatments up to 900 K. These results offer good prospects for the use of the $ThMn_{12}$ nitrides as bulk magnets provided an adequate processing route is found.

II. EXPERIMENTAL DETAILS

Flakes with a nominal composition $(Nd_{0.75}, Pr_{0.25})_{1.2}Fe_{10.5}Mo_{1.5}$ were prepared by the strip cast method using metals with purity >99.9%. An excess of (Nd,Pr) mixture (20 at.%) was added in order to enhance the hard magnetic properties [15,20]. The obtained alloys were then melt-spun by ejecting the molten alloy through an orifice (0.8 mm) from the bottom of a quartz tube onto a copper wheel under argon atmosphere. The linear wheel velocity (v) was fixed to 25 m/s. The quenching rate was optimized to obtain a pure $ThMn_{12}$ structure with the finest microstructure possible, i.e., about 200 nm in grain size. The ribbons were crushed into powder (<40 μm) and then nitrogenated at 873 K for 3 hours under a N_2 atmosphere, as described previously [15]. To investigate the thermostability of the magnetic properties, the nitride powder was sealed in quartz ampoules under vacuum, and then heat treated at various temperatures between 873 and 973 K for 30 min followed by quenching in air.

The crystal structures of the non-nitride and nitride powders were determined by x-ray diffraction (XRD) using Cu $K\alpha$ radiation. Magnetic measurements were performed using 2 T (Microsense) and 14 T (Quantum Design) vibrating sample magnetometers (VSMs). Powder neutron diffraction experiments were carried out at the diffractometer D1B, ILL (Institut Laue-Langevin, France) using a calibrated wavelength of $\lambda = 2.5219$ Å. The measurements were performed on ground powders obtained from the ribbons and a random orientation was ensured during the experiment. The diffractograms were taken at different temperatures ranging from 300 to 1010 K under a high vacuum of approximately 10^{-5} mbar. The crystal structure was refined using the Rietveld method implemented in the FULLPROF program [21]. The magnetic scattering contribution was taken into account in the refinement and the magnetic structure was calculated using the MAXMAGN program [22].

III. RESULTS AND DISCUSSION

A. Preliminary structural and magnetic properties

The XRD patterns of the compounds before and after nitrogenation are plotted in Fig. 1. Both samples show a quasipure $ThMn_{12}$ structure with a small amount (<2 wt.%) of impurities, mostly α-(Fe,Mo) and a few traces of metallic Nd (dhcp). For the nitrides, we observe a shift of the peak positions to lower angles, owing to the nitrogen inclusion in the 2b site of the lattice, resulting in an increase of both the a and c cell parameters [15].

The magnetic hysteresis loops with fields up to 4 T are shown in Fig. 2. The saturation magnetization is reached for the parent compound, giving a value $M_s = 90$ Am^2/kg, which is consistent for Nd-Fe-Mo alloys [15]. For the nitrides, the saturation is not reached at 4 T. However, this field is high enough to observe a coercive field >0.5 T, suggesting a proper nitrogenation and proving its effect on the anisotropy of these compounds.

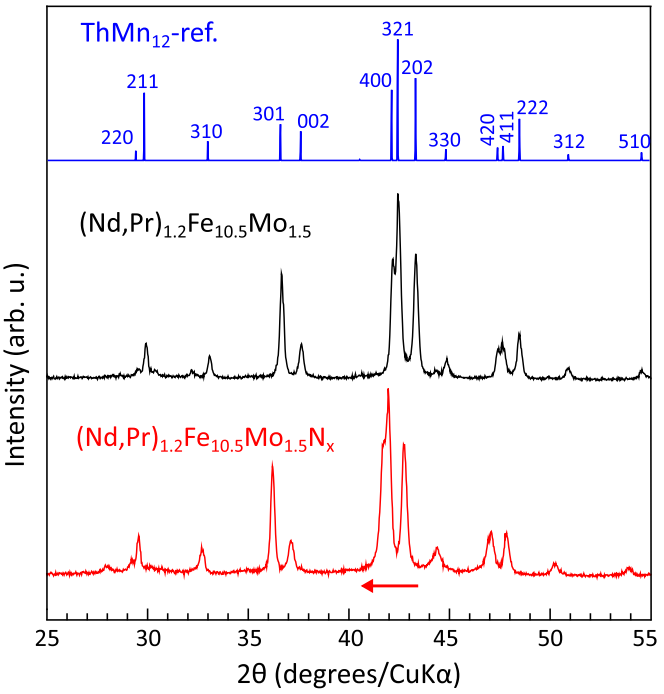

FIG. 1. XRD patterns obtained before and after nitrogenation of $(Nd_{0.75}, Pr_{0.25})_{1.2}Fe_{10.5}Mo_{1.5}$ together with a reference pattern of the $ThMn_{12}$ phase.

Thermomagnetic measurements $M(T)$ were also conducted for both samples (see Fig. 3). The as-spun ribbons have a Curie temperature (T_C) of approximately 465 K, which is in agreement with those reported for such compounds [15,23]. As expected, an efficient nitrogenation leads to an increase of the Curie temperature (up to 625 K here) mostly due to the enhancement of the Fe-Fe interactions, which results from

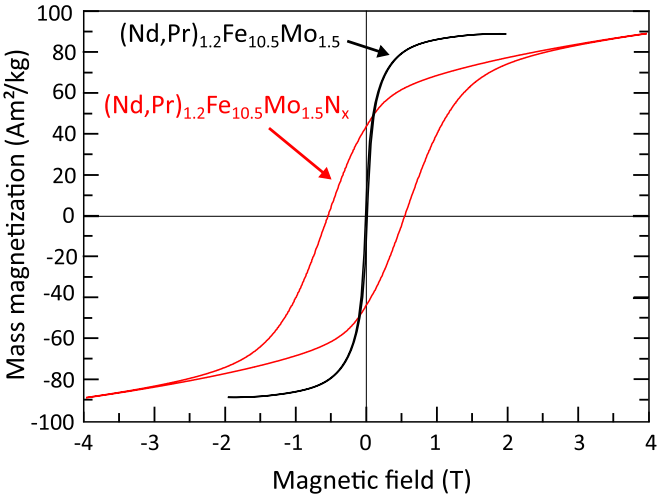

FIG. 2. Magnetic hysteresis loops obtained before and after nitrogenation of $(Nd_{0.75}, Pr_{0.25})_{1.2}Fe_{10.5}Mo_{1.5}$.

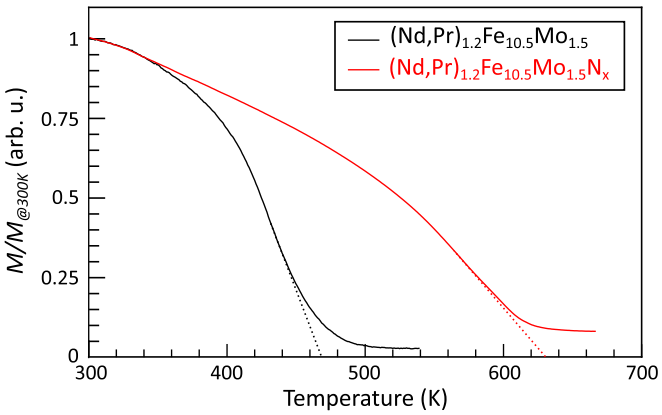

FIG. 3. Thermal-magnetization curves of $(Nd_{0.75}, Pr_{0.25})_{1.2}Fe_{10.5}Mo_{1.5}$ before and after nitrogenation measured at $H = 500$ Oe. A straight line (dotted) is drawn at the maximum curvature point to estimate the Curie temperature.

the inclusion of the N element in the interstitial 2b site of the $ThMn_{12}$ structure [15].

B. Powder neutron diffraction

1. *Parent compound:* $(Nd_{0.75}, Pr_{0.25})_{1.2}Fe_{10.5}Mo_{1.5}$

Powder neutron diffraction measurement of the parent compound was first performed at room temperature in order to investigate the $ThMn_{12}$ structure of the $(Nd_{0.75}, Pr_{0.25})_{1.2}Fe_{10.5}Mo_{1.5}$ as-spun powder, which is shown in Fig. 4. Rietveld refinement of the neutron diffraction confirms the tetragonal structure ($I4/mmm$) with a lattice

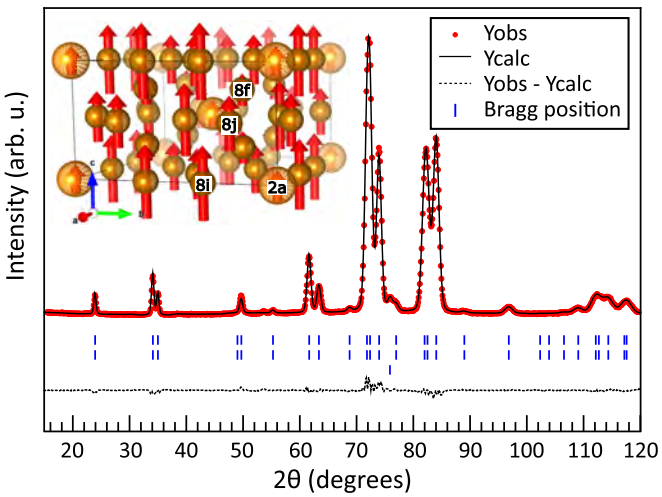

FIG. 4. Plot of the Rietveld refinement of the powder neutron diffraction pattern recorded at room temperature for $(Nd_{0.75}, Pr_{0.25})_{1.2}Fe_{10.5}Mo_{1.5}$. The red points are experimental data and the black line corresponds to the Rietveld fit. The first and second blue rows of the Bragg peak positions refer to the nuclear and magnetic contributions of the $ThMn_{12}$, respectively. The third blue row refers to the nuclear contribution of α-(Fe,Mo) phase. The dashed line is the difference between the observed and calculated patterns. The inset shows the $ThMn_{12}$ crystal structure with the atomic magnetic moments.

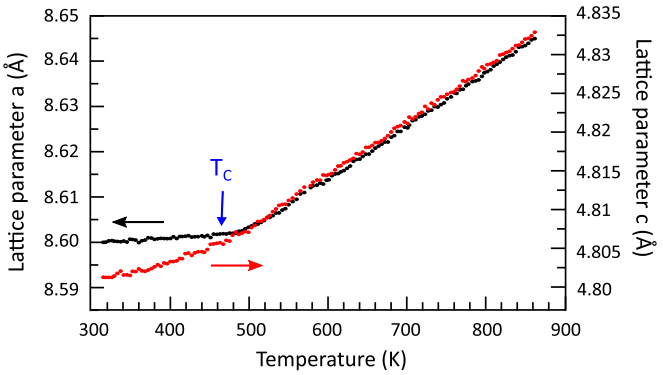

FIG. 5. Temperature dependence of lattice parameters a (left, black) and c (right, red) obtained by Rietveld refinements of $(Nd_{0.75}, Pr_{0.25})_{1.2}Fe_{10.5}Mo_{1.5}$ measured by powder neutron diffraction.

parameters $a = 8.600(5)$ Å, $c = 4.802(4)$ Å, a ratio c/a of 0.558, and a volume cell (Vol.) of 355.2(3) Å^3. The Mo element shares the 8i site with Fe, as observed in Mössbauer spectroscopy [15]. In addition to the $ThMn_{12}$ structure, traces (1.42 wt.%) of α-(Fe,Mo) phase are also detected, with a lattice parameter $a = 2.901(4)$ Å.

The magnetic space group $I4/mm'm'$ (139.537) in the BNS notation is used to describe the magnetic structure. The magnetic moments are along the c axis (as shown in the inset of Fig. 4) and their values are reported in Table II. A clear tendency in the order of the iron moment shows $\mu_{8i} > \mu_{8j} > \mu_{8f}$. The magnetic moment per unit cell is estimated to be $25.613\mu_B$, giving a spontaneous mass magnetization of 80.8 Am^2/kg. This is slightly lower than the spontaneous magnetization measured for $(Nd_{0.75}, Pr_{0.25})_{1.2}Fe_{10.5}Mo_{1.5}$ at 300 K, but still in good agreement if considering the standard deviation of the magnetic moments. Moreover, the moments obtained here are extremely sensitive to other refinements parameters. The fitting presents a reliability factor of $\chi^2 = 2.8$ with nuclear and magnetic R factors of 2.41 and 2.10, respectively.

Then, thermodiffractograms were acquired while the powder was heated at 2 K/min up to 880 K. No change in the magnetic structure was observed during the heating, and the magnetic moment at each site decreases uniformly with temperature. The evolution of a and c lattice parameters as a function of the temperature is plotted in Fig. 5. Both lattice parameters exhibit a different linear thermal expansion in the ferromagnetic and paramagnetic regimes. Below the Curie temperature, there is almost no thermal expansion for the lattice parameter a. This anomaly in the a-b plane has also been observed in other $ThMn_{12}$ alloys [24–27]. For some of these compounds, a negative lattice thermal expansion was reported just before T_C, which is not observed here. It seems that such irregularity is linked to the rare-earth elements (Nd, Ce, Pr, etc.) and the transition metals (Ti, V, Mo, etc.) used to stabilize the structure. To the best of our knowledge, no negative thermal expansion has been reported above 300 K for the Nd-based $ThMn_{12}$ compound stabilized by the Mo transition metal, which is in agreement with our observations. However, it seems that such an anomaly is present below

TABLE I. Cell parameters of the $ThMn_{12}$ phase obtained after the Rietveld refinements for the parent compound and its corresponding nitride, using powder neutron diffraction at 300 K. For $(Nd_{0.75}, Pr_{0.25})_{1.2}Fe_{10.5}Mo_{1.5}$, the parameters are also given at 873 K, which is the temperature used for nitrogenation.

	$(Nd_{0.75}, Pr_{0.25})_{1.2}Fe_{10.5}Mo_{1.5}$		$(Nd_{0.75}, Pr_{0.25})_{1.2}Fe_{10.5}Mo_{1.5}N_{0.85}$
	300 K	873 K	300 K
a (Å)	8.600(5)	8.644(3)	8.668(5)
c (Å)	4.802(4)	4.834(4)	4.871(9)
c/a	0.558(3)	0.559 (3)	0.562(0)
Vol. (Å^3)	355.2(3)	361.2(5)	366.0(9)
$\Delta V/V$ (%)		1.694(7)	3.057(2)
Cryst. size (nm)	64	79	50

room temperature [28]. Above the Curie temperature, both the a and c lattice parameters exhibit a quasilinear regime and a similar thermal expansion of $\alpha_a = 1.37 \times 10^{-5}$ K^{-1} and $\alpha_c = 1.44 \times 10^{-5}$ K^{-1}, respectively. These values are consistent with previous studies [26,29]. Thus, there is a strong correlation between the thermal dilatation exhibited by the crystal structure and the magnetic state (ferromagnetic or paramagnetic) of the compounds.

The lattice parameters and cell volume obtained at the temperature used for the nitrogenation process (i.e., 873 K), are listed in Table I. At this particular temperature, the lattice parameters a and c increase by 0.51% and 0.67%, respectively, with respect to room temperature, thus leading to a volume expansion of 1.69%. It is interesting to note that the expansion seems to be isotropic and the structure remains stable in a large temperature range.

2. *Nitrides:* $(Nd_{0.75}, Pr_{0.25})_{1.2}Fe_{10.5}Mo_{1.5}N_{0.85}$

To evaluate accurately the structural changes induced by the nitrogen inclusion, the $(Nd_{0.75}, Pr_{0.25})_{1.2}Fe_{10.5}Mo_{1.5}N_x$ powder was first measured at room temperature, and the neutron diffraction pattern is shown in Fig. 6. Unlike x rays, neutrons are sensitive to light elements; the relative intensities of the pattern are thus correlated to the nitrogen content in the structure. The diffraction pattern obtained after nitrogenation is hence different than for the parent compound. Here, the number of nitrogen atoms per formula unit is estimated to be $x = 0.85$. The values of the lattice parameters for the $ThMn_{12}$ structure of the parent and nitrogenated samples are summarized in Table I. Compared to the parent compound, we note increases of 0.79%, 1.44%, 0.71%, and 3.07% for the lattice parameters a and c, the c/a ratio, and the volume (Vol.), respectively. The nitrogenation induces a quasi-isotropic expansion of the unit cell volume, with a slightly greater increase in the c axis compared to the a axis, which is correlated with the $4f$ electron states of the rare-earth elements [7]. One can also note a decrease of the average crystallite size for the nitrides compared to the parent compound (see Table I). This effect can be attributed to the nature of the nitrogenation process, which introduces a large change in cell volume that can lead to stresses inducing grain breaking, hence reducing the average crystallite size. On the other hand, the presence of non-nitrogenated crystallites in the nitrogenated compound might lead to a broadening of the diffraction peaks, which can be misinterpreted as a reduction in size. In addition to the $ThMn_{12}$ structure, a small amount (3.11 wt.%) of α-(Fe,Mo) is also detected, with a lattice parameter $a = 2.895(2)$ Å. The peak observed at $2\theta = 58.75^\circ$ is attributed to traces of NdN or PrN.

For the nitrides, we also used the magnetic space group $I4/mm'm'$ (139.537) in the BNS notation to describe the magnetic structure. The magnetic moments are along the c axis (as shown in the inset of Fig. 6) and their values are reported in Table II. The magnetic moments are increased after nitrogenation and the tendency in the order of the iron moment is maintained: $\mu_{8i} > \mu_{8j} > \mu_{8f}$. The increase of the iron moments explains the increase in Curie temperature observed in the nitrides. The magnetic moment per unit cell is estimated to be $37.67\mu_B$, giving a spontaneous mass magnetization of 118.51 Am^2/kg, in agreement with the magnetic measurements [15]. The refinement presents a reliability factor of $\chi^2 = 4.44$ with nuclear and magnetic R factors of 2.86 and 2.17, respectively.

To study the *in situ* denitrogenation process of the nitrides, powder neutron diffraction was performed by heating

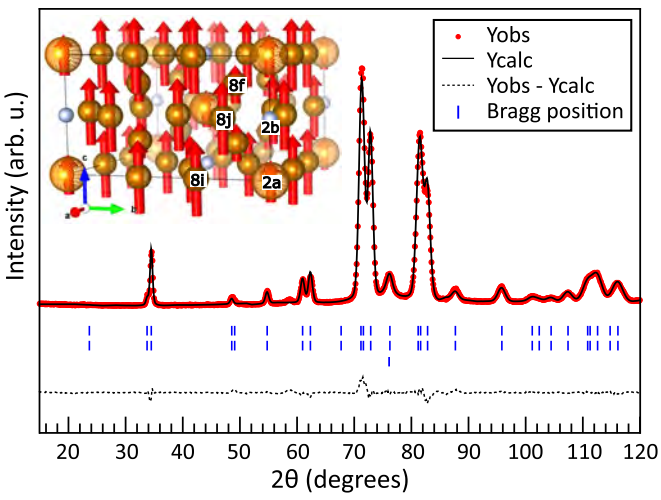

FIG. 6. Plot of the Rietveld refinement of the powder neutron diffraction pattern recorded at room temperature for the nitride $(Nd_{0.75}, Pr_{0.25})_{1.2}Fe_{10.5}Mo_{1.5}N_{0.85}$. The first and second blue rows of the Bragg peak positions refer to the nuclear and magnetic contributions of the $ThMn_{12}$, respectively. The third blue row refers to the nuclear contribution of the α-(Fe,Mo) phase. The inset shows the $ThMn_{12}$ crystal structure with the atomic magnetic moments.

TABLE II. Magnetic moments of $(Nd_{0.75}, Pr_{0.25})_{1.2}Fe_{10.5}Mo_{1.5}$ and $(Nd_{0.75}, Pr_{0.25})_{1.2}Fe_{10.5}Mo_{1.5}N_{0.85}$ obtained by neutron diffraction at 300 K (unit: μ_B).

Atom	Site	$(Nd_{0.75}, Pr_{0.25})_{1.2}Fe_{10.5}Mo_{1.5}$	$(Nd_{0.75}, Pr_{0.25})_{1.2}Fe_{10.5}Mo_{1.5}N_{0.85}$
Nd, Pr	2a	0.702 (116)	1.173 (123)
Fe	8i	1.737 (128)	2.128 (137)
Fe	8j	1.249 (107)	2.051 (88)
Fe	8f	0.765 (116)	1.124 (89)

the powder at 2 K/min until reaching 873 K. Then, the powder was maintained at this temperature for 3 hours, i.e., using the same temperature profile as in the nitrogenation process [15]. Finally, the temperature was further increased to 1010 K. This process was performed under high vacuum (10^{-5} mbar). No change in the magnetic structure was observed during the heating, and the magnetic moment at each site decreases uniformly with temperature. Cyclic refinement of the obtained diffractograms measured at different temperatures was performed by FULLPROF SUITE, and the resulting values of the cell volume of the $ThMn_{12}$ at these temperatures are shown in Fig. 7. On the same figure, the mass fraction of the secondary phase α-(Fe,Mo) is also plotted, together with the number of nitrogen atoms per formula unit in the $(Nd_{0.75}, Pr_{0.25})_{1.2}Fe_{10.5}Mo_{1.5}N_x$ compound, which is estimated based on the occupancy of the nitrogen atoms.

After the "nitrogenation-like" process (i.e., ramped to 873 K and maintained for 3 hours at this temperature), a quasilinear volume expansion with respect to the temperature is observed (see Fig. 7). On the other hand, the amount of the secondary phase α-(Fe,Mo) remains stable as well as the atomic occupancy of the nitrogen within the lattice. Previous *in situ* neutron diffraction studies regarding the nitrogenation process reported that the nitrogen usually starts entering in the lattice before the temperature reaches its optimum value [11,12]. Regarding denitrogenation, the process is completely different, as we observe an excellent stability of the nitrogen in the lattice and hence of the $ThMn_{12}$ structure. It should be highlighted that the denitrogenation process is performed under high vacuum (10^{-5} mbar), which seems to help in the stability of the nitrogen atom, in contrast to the denitrogenation process under air, known to form Fe-based oxides [15]. Here, the formation of α-(Fe,Mo) is significantly increased around 930 K, which also corresponds to the temperature at which the nitrogen occupancy starts to decrease.

After reaching 1010 K, the heating was stopped and the pattern was recorded while the sample was cooled down. In total, the sample was kept 3 hours at 873 K and more than 1 hour above this temperature. The pattern of the sample recorded at 370 K while cooling down is shown in Fig. 8. The pattern consists of mainly three phases: the $ThMn_{12}$ (47.5 wt.%), α-(Fe,Mo) (50 wt.%), and NdN (2.5 wt.%). The amount of nitrogen remaining in the lattice at the end of the experiment was still 0.54 at/f.u. Hence, it seems that nitrogen is very stable in the lattice and that the decomposition is mainly due to the formation of the secondary α-(Fe,Mo) phase, which appears to be faster than the nitrogen losses in the lattice. This was also suggested in previous studies based on Differential thermal analysis (DTA)/Thermogravimetric analysis (TG)/XRD investigations of Nd-based nitrides [18,30]. The good stability of the nitrides at elevated temperatures is mostly

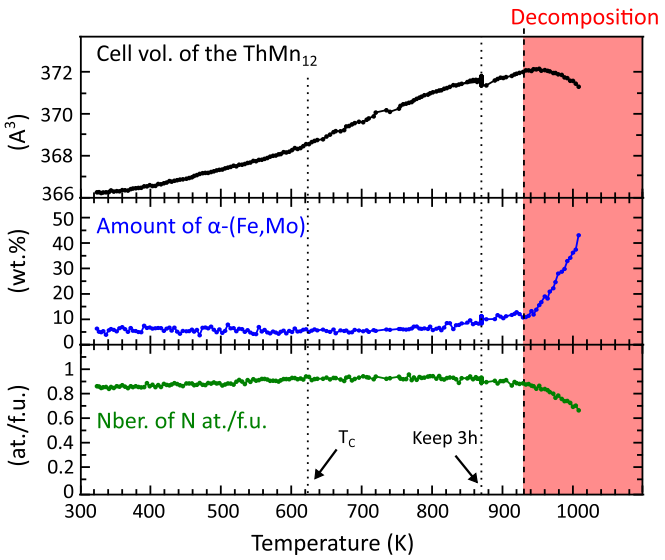

FIG. 7. Thermal evolution of the cell volume of the $ThMn_{12}$ (top, black line); mass fraction of the secondary phase α-(Fe,Mo) (center, blue line), and occupancy of nitrogen atoms (bottom, green line) obtained by Rietveld refinements of the $(Nd_{0.75}, Pr_{0.25})_{1.2}Fe_{10.5}Mo_{1.5}N_x$ neutron diffraction.

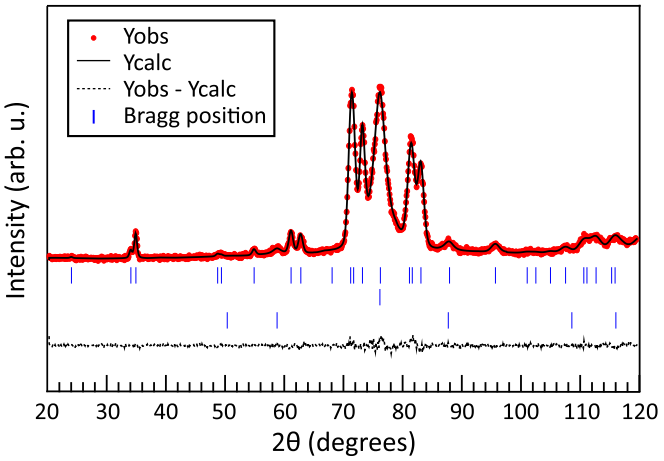

FIG. 8. Plot of the Rietveld refinement of the powder neutron diffraction pattern recorded at 370 K for $(Nd_{0.75}, Pr_{0.25})_{1.2}Fe_{10.5}Mo_{1.5}N_{0.54}$ after heating up to 1010 K. The first, second, and third blue rows refer to the Bragg peak positions of the $ThMn_{12}$, α-(Fe,Mo), and NdN phases respectively.

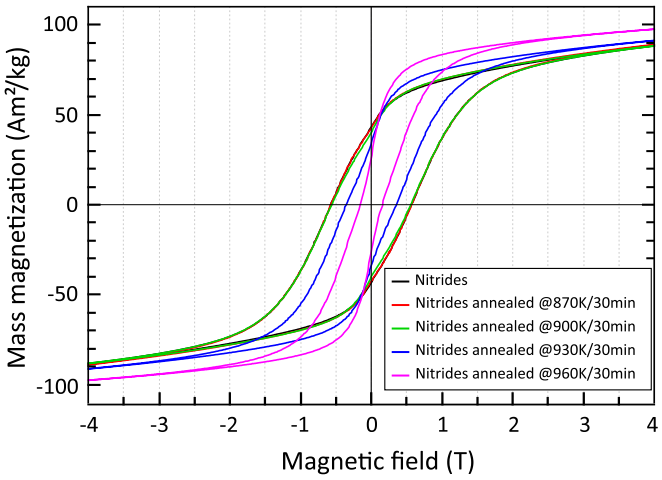

FIG. 9. Magnetic hysteresis loops of the nitrides $(Nd_{0.75}, Pr_{0.25})_{1.2}Fe_{10.5}Mo_{1.5}N_x$ after being heat treated at different temperatures.

due to the transition element used, i.e., Mo, which allows a much better thermal stability than Ti or V [18].

C. Magnetic properties after thermal treatment

As the α-(Fe,Mo) continuously increases between 870 and 930 K, it was not clear how this could affect the magnetic properties of the nitrides. Thus, the nitrogenated samples were annealed in vacuum at 870, 900, 930, and 960 K for 30 min and their magnetic properties were investigated after this thermal treatment. The M-H loops measured for the heat-treated compounds are plotted in Fig. 9. The nitrides maintained their good magnetic properties after being heated up to 900 K. Above this temperature, the coercive field starts to decrease rapidly, reaching 0.15 T after a heat treatment at 960 K. On the other hand, the saturation magnetization is slightly increased. The changes in H_c and M_s are attributed to the formation of α-(Fe,Mo) as observed in the neutron powder diffractograms. This result indicates a good prospect to possibly sinter this compound by reducing the sintering temperature below 930 K. This is possible using nonconventional sintering techniques such as spark plasma sintering or hot pressing [17,30–33]. The nitrides could also be good candidates for additive manufactured magnets [34].

IV. CONCLUSION

In summary, we have investigated the structural and magnetic properties of the $(Nd_{0.75}, Pr_{0.25})_{1.2}Fe_{10.5}Mo_{1.5}N_x$ compound. The structural properties were investigated by means of powder neutron diffraction measurements performed at different temperatures for the parent compounds and their corresponding nitrides. After nitrogenation, the unit cell volume expansion due to the inclusion of N in the 2b site is isotropic. The heating of the nitrides shows that the denitrogenation process is different from the nitrogenation, as the atomic site occupancy of the nitrogen in the lattice is stable until approximately 930 K. Above this temperature, the formation of α-(Fe,Mo) rapidly increases, which results in the loss of nitrogen. The nitrides maintained their good magnetic properties after being heated up to 900 K, in agreement with the structural study performed by neutron diffraction. This result offers future prospects to use this compound for sintered permanent magnets.

ACKNOWLEDGMENTS

The authors acknowledge the project "SpINS: Spanish Initiatives on Neutron Scattering," funded by the Spanish Ministry of Science and Innovation, and the CSIC for the neutron beam time granted on the "CRG-D1B." Institut Laue-Langevin (ILL) is also acknowledged [35]. We are also thankful for technical and human support provided by SGIker (UPV/EHU) and particularly the services of X-Ray Molecules and Materials (Dr. Aitor Larrañaga Varga) and Magnetic Measurements (Dr. Iñaki Orue). This work has received funding from the European Union's Horizon 2020 research and innovation program under Grant Agreement No. 686056 (NOVAMAG).

[1] J. Cui, M. Kramer, L. Zhou, F. Liu, A. Gabay, G. Hadjipanayis, B. Balasubramanian, and D. Sellmyer, Acta Mater. **158**, 118 (2018).
[2] K. P. Skokov and O. Gutfleisch, Scr. Mater. **154**, 289 (2018).
[3] J. Coey, Engineering **6**, 119 (2020).
[4] F. Maccari, L. Schäfer, I. Radulov, L. Diop, S. Ener, E. Bruder, K. Skokov, and O. Gutfleisch, Acta Mater. **180**, 15 (2019).
[5] D. Niarchos, M. Gjoka, A. M. Schönhöbel, A. Aubert, R. Madugundo, J. J. S. Garitaonandía, J. M. Barandiaran, and G. Hadjipanayis, J. Alloys Compd. (2020), doi: 10.1016/j.jallcom.2020.158097.
[6] D. P. F. Hurley and J. M. D. Coey, J. Phys.: Condens. Matter **4**, 5573 (1992).
[7] T. Zhao, X. C. Kou, Z. D. Zhang, X. K. Sun, Y. C. Chuang, and F. R. de Boer, J. Phys.: Condens. Matter **8**, 8923 (1996).
[8] J. Coey, H. Sun, and D. Hurley, J. Magn. Magn. Mater. **101**, 310 (1991).
[9] J. Coey, J. Magn. Magn. Mater. **159**, 80 (1996).
[10] P. Oleinek, D. Eckert, K.-H. Müller, and L. Schultz, J. Phys. D: Appl. Phys. **32**, 1578 (1999).
[11] C.-K. Loong, S. M. Short, J. Lin, and Y. Ding, J. Appl. Phys. **83**, 6926 (1998).
[12] P. Oleinek, O. Isnard, P. Convert, K.-H. Müller, M. Loewenhaupt, and L. Schultz, J. Alloys Compd. **298**, 220 (2000).
[13] I. Popa, S. Rivoirard, P. de Rango, and D. Fruchart, J. Alloys Compd. **428**, 44 (2007).
[14] Z. Lin, J. Han, S. Liu, M. Xing, Y. Yang, J. Yang, C. Wang, H. Du, and Y. Yang, J. Magn. Magn. Mater. **324**, 196 (2012).

[15] A. Aubert, R. Madugundo, A.-M. Schönhöbel, D. Salazar, J.-S. Garitaonandia, J.-M. Barandiaran, and G. Hadjipanayis, Acta Mater. **195**, 519 (2020).
[16] A. Gabay and G. Hadjipanayis, Scr. Mater. **154**, 284 (2018).
[17] J.-M. Barandiaran, A. Martin-Cid, A.-M. Schönhöbel, J.-S. Garitaonandia, M. Gjoka, D. Niarchos, S. Makridis, A. Pasko, A. Aubert, F. Mazaleyrat, and G. Hadjipanayis, J. Alloys Compd. **784**, 996 (2019).
[18] K. Kobayashi, D. Furusawa, S. Suzuki, T. Kuno, K. Urushibata, N. Sakuma, M. Yano, T. Shoji, A. Kato, A. Manabe, and S. Sugimoto, Mater. Trans. **59**, 1845 (2018).
[19] K. Binnemans, P. Jones, T. Müller, and L. Yurramendi, J. Sustain. Metall. **4**, 126 (2018).
[20] F. E. Pinkerton, C. D. Fuerst, and J. F. Herbst, J. Appl. Phys. **75**, 6015 (1994).
[21] J. Rodriguez-Carvajal, Phys. B **192**, 55 (1993).
[22] J. Perez-Mato, S. Gallego, E. Tasci, L. Elcoro, G. de la Flor, and M. Aroyo, Annu. Rev. Mater. Res. **45**, 217 (2015).
[23] M. Endoh, K. Nakamura, and H. Mikami, IEEE Trans. Magn. **28**, 2560 (1992).
[24] K. Buschow, J. Less Common Metals **144**, 65 (1988).
[25] J. Wang, C. Marquina, B. Garcia-Landa, M. Ibarra, F. Yang, and G. Wu, Phys. B **319**, 73 (2002).
[26] D. Salazar, A. Martín-Cid, J. Garitaonandia, T. Hansen, J. Barandiaran, and G. Hadjipanayis, J. Alloys Compd. **766**, 291 (2018).
[27] W. Li, K. Lin, Y. Cao, C. Yu, C.-W. Wang, X. Liu, K. Kato, Y. Wang, J. Wang, Q. Li, J. Chen, J. Deng, H. Zhang, and X. Xing, CCS Chemistry (2020), doi:10.31635/ccschem.020.202000279.
[28] L. Junhong, L. Yuntao, L. Tianfu, Z. Li, H. Wenze, G. Jianbo, C. Dongfeng, and D. Honglin, At. Energy Sci. Technol. **46**, 23 (2012).
[29] H. Sun, M. Akayama, K. Tatami, and H. Fujii, Physica B **183**, 33 (1993).
[30] J. Kong, C. Zhou, and F. E. Pinkerton, IEEE Trans. Magn. **52**, 1 (2016).
[31] T. Saito and K. Kikuchi, J. Alloys Compd. **673**, 195 (2016).
[32] T. Saito, F. Watanabe, and D. Nishio-Hamane, J. Alloys Compd. **773**, 1018 (2019).
[33] A.-M. Schönhöbel, R. Madugundo, A. Gabay, J. Barandiaran, and G. Hadjipanayis, J. Alloys Compd. **791**, 1122 (2019).
[34] K. Gandha, L. Li, I. Nlebedim, B. K. Post, V. Kunc, B. C. Sales, J. Bell, and M. P. Paranthaman, J. Magn. Magn. Mater. **467**, 8 (2018).
[35] Institut Laue-Langevin, doi:10.5291/ILL-DATA.CRG-2659.